

# Wind-Induced Interference Effects on a 125 m Tall RC Chimney in Typical Power Plant



G. Ramesh Babu, Ramya Niranjana, and A. Abraham

**Abstract** This paper presents the details of the wind tunnel investigations carried out on the aeroelastic behaviour of a tall RC chimney in the presence of surrounding structures for two typical power plant layouts in India. The RC chimney under investigation considered as a principal chimney has uniform diameter of 10.41 m and height of 124.5 m. The surrounding structures include 275 m tall chimney considered as interfering chimney and other power plant structures with the c/c distance-to-diameter ratio of 16 (layout-1) and 25 (layout-2) between principal chimney and interfering chimney. Experiments were conducted on the models with a geometric scale of 1:250 under simulated boundary layer conditions in the wind tunnel facility at CSIR-SERC, Chennai. Both the layouts are tested for various wind incidence angles and reduced velocity ( $\bar{U}/n_0D$ ) ranges from 1.8 to 6.56. From the previous research works carried out, the magnification factor was observed to be maximum when the principal chimney is in downstream and interfering chimney is at  $0^\circ \pm 15^\circ$ . In this work, the maximum magnification factor was noticed to occur when the interfering chimney is at  $15^\circ, 180^\circ, 210^\circ$  for layout-1 and  $35^\circ, 65^\circ, 320^\circ$  for layout-2. In addition to the magnification factor, the variation of maximum interference factor for the resultant bending moment at critical wind speed with respect to the angle wind incidence was also discussed.

**Keywords** Wind tunnel test · Interference effects · RC chimneys · Aeroelastic response · Magnification factor

## 1 Introduction

It is important to understand the dynamic response of wind-sensitive structures such as tall chimneys as complex fluid–structure interactions are expected to occur when subjected to wind loads. In a typical thermal power plant, a chimney is seldom in

---

G. Ramesh Babu · R. Niranjana (✉) · A. Abraham

Wind Engineering Laboratory, CSIR—Structural Engineering Research Centre, Chennai, India  
e-mail: [ramya@serc.res.in](mailto:ramya@serc.res.in)

© The Author(s), under exclusive license to Springer Nature Singapore Pte Ltd. 2024  
S. G. Rajasekharan et al. (eds.), *Proceedings of the 9th National Conference on Wind Engineering*, Lecture Notes in Mechanical Engineering,  
[https://doi.org/10.1007/978-981-99-4183-4\\_13](https://doi.org/10.1007/978-981-99-4183-4_13)

133

stand-alone condition and is usually surrounded by other structures, viz., similar or dissimilar chimneys, cooling towers, boiler and bunker buildings, etc. The complexity in flow mechanism and associated fluid–structure interaction increases manifold due to change in flow field caused by these surrounding structures. This phenomenon is termed as wind-induced interference effects which should be accounted during the design of chimneys.

The wind-induced behaviour of circular cylinders has importance in many engineering applications and has been studied extensively by many researchers. The presence of neighbouring structures/cylinders introduces interference effects either through shielding or enhancement on loads. Several researchers, starting with the pioneering work of Zdravkovich [1], have studied the effects of wind-induced interference effects between group of cylinders. Sets of two-, three-pipe clusters, square and irregular multi-pipe clusters with pipes of same diameter subjected to flow conditions are studied to obtain the variation of lift and drag coefficients. Based on a series of experiments, Zdravkovich classified three regions for the purpose of studying flow interference between two cylinders as (a) proximity, (b) wake and (c) no interference regions. Wind tunnel experiments were carried out by Gowda et al. [2] on two circular cylinders with varying diameter ratios for different arrangements (tandem, staggered and side-by-side). It was inferred that the tandem arrangement was critical as peak response in interference condition increased by 2–3 times compared to the isolated case. Wind tunnel investigations of interference effects between two and three cylinders of equal diameter of finite height were carried out by Kareem et al. [3] in simulated boundary layer conditions in both tandem and side-by-side configurations. The variation of force coefficients with respect to different arrangements, spacing of cylinders and wind incident angles was discussed. Pressure distributions on two circular cylinders in staggered arrangement with aspect ratio of 6.4 were reported by Gu and Sun [4]. From their study, they have classified the pressure pattern distribution into three groups corresponding to various angles of attack. Interference effect of two-, three- and four-cylinders of varying diameters (6, 8.9 and 12.2 cm) arranged in-line was investigated by Liu et al. [5] through wind tunnel tests. The change in mean force coefficients for different spacings, smooth and turbulent flow conditions, surface roughness and Reynolds numbers were discussed in detail.

Following the studies on group effects of uniform circular cylinder at subcritical flow conditions, research activities on understanding the interference effects between tall chimneys subjected to boundary layer flow were extensively carried out. Wind tunnel experiments were performed by Niemann and Kasperski [6] on two 200 m reinforced concrete (RC) chimneys of 20 m diameter subjected to  $0^{\circ}$ – $30^{\circ}$  angle of attack. They opined that the interference leads to mixed excitation besides resonance due to the turbulence of the oncoming flow, and considerable resonance excitation may occur due to wake buffeting for chimneys with high natural frequencies. Aeroelastic model of 100 m tall chimney with surrounding chimneys and buildings was tested in wind tunnel by John et al. [7]. The across-wind response was found to be predominant and was two times higher in interference condition compared to isolated condition. The reduction in response due to the influence of stakes has also been discussed. Interference effects were studied for two 200 m tall chimneys using

rigid model in wind tunnel by Sun et al. [8]. Pressure distribution was obtained for various angles of attack ranging from  $0^\circ$  to  $180^\circ$  and spacing-to-diameter ratios of 2–6. Critical angles of attack and spacing ratios were identified, and it was also observed that across-wind response was predominant. This work was followed by performing experimental tests on aeroelastic model of tall chimneys by Su et al. [9] for the critical angles of attack and spacings. For spacing-to-diameter ratios of 3–6, response is influenced by vortex shedding due to upstream chimney, and for ratio less than 2, gap flow was found to dominate the response. In addition, the experimental values with ACI 307-08 standard [10] was also compared. Three different groups of two tall chimneys with combination of straight, 1:40 and 1:50 taper cylinders were tested by Rajora et al. [11] to compare the along- and across-wind responses. The results were compared with various codes for spacing-to-diameter ratios greater than 15. The magnification factors were found to be greater than 1 even for higher spacing to diameter ratios ( $>35$ ).

From the previous research works conducted, it is evident that the wind-induced interference effects have been mostly studied for identical cylinders/chimneys with same height and diameter and the interfering cylinder placed in tandem, staggered or side-by-side positions. In a thermal power plant layout, these typical cases may not be directly applicable to obtain responses of tall chimneys. In this work, we have considered dimensions of tall chimneys from a typical power plant layout to understand the wind-induced interference effects. The effect of 275 m tall RC chimney with base diameter of 30 m and having tapering for the bottom 40% of the height (interfering chimney) and surrounding building structures on a 124.5 m tall uniform diameter (10.41 m) RC chimney (principal chimney) for two different layouts are investigated using wind tunnel experiments. The *c/c* distance-to-diameter (*S/D*) ratio is 16 for layout-1 and 25 for layout-2. The location and orientation of surrounding structures are different in two layouts as in a typical power plant.

## 2 Wind Tunnel Test Setup

Experiments are performed in open circuit and blower-type boundary layer wind tunnel having test section of dimensions 2.5 m (*W*)  $\times$  2.0 m (*H*)  $\times$  18.0 m (*L*) at CSIR-SERC, India. It is possible to satisfactorily generate a boundary layer depth of about 1.20 m in the test section corresponding to open terrain conditions. Since the model of the chimney is to be fully immersed within the boundary layer as per similarity requirements, a scale of 1:250 was selected in the present study. The aeroelastic model of the principal chimney is fabricated using aluminium, and the resulting model dimensions to a geometric scale of 1:250 is 498 mm height, 41.64 mm diameter and 1.6 mm thickness. The interfering chimney is also scaled down as rigid model is made of wood material with a height of 1100 mm. The models of surrounding building structures are fabricated with acrylic sheets. The principal chimney is mounted at the centre of the turntable whose diameter is about 2.4 m.

Wind tunnel tests are conducted under simulated wind characteristics pertaining to open terrain category as per Indian Standard (IS) 875 (Part 3):2015 [12]. The required wind characteristics are achieved using a trip board and wooden panels containing roughness cubes in the test section. The typical power law coefficient for open terrain condition as per IS 875 (Part 3):2015 of 0.16 is also experimentally accomplished. Furthermore, the turbulence intensity is also achieved as per the IS code. The power spectrum of longitudinal fluctuating component of wind speed simulated is found to be in good agreement with the von Karman spectrum.

Tests are conducted for a range of mean wind speeds between 8.78 and 32.2 m/s measured at top of principal chimney model (498 mm). The mean wind speeds during the tests are measured using pitot-static tube whose static and total are connected to a 2480 Pa pressure scanner. Strain gauge instrumentations are adopted on the aeroelastic model of the principal chimney with strain gauge channels in two orthogonal directions at four locations, at base (0.0241 H), 0.25 H, 0.5 H and 0.75 H, where H is the height of the chimney, to measure the bending moments (BMs) at these levels. For each channel, full bridge circuitry is used with four strain gauges having a resistance of 120  $\Omega$  and gauge factor of  $2.13 \pm 1\%$ . The strain gauge channels are calibrated using standard dead weights. Additionally, the model is instrumented with two accelerometers at the top in orthogonal directions to measure tip accelerations. The data are acquired with a sampling frequency of 1200 samples/s and a sampling duration of 15 s. For each wind speed, data are acquired for three trials.

Experimental investigations are carried out in three stages. Firstly, the principal chimney is tested in stand-alone condition subjected to 13 different wind speeds having mean wind velocities between 8.78 and 32.2 m/s. These wind velocities correspond to a reduced velocity  $\bar{U}/n_0D$  of 1.79–6.55. Following which, tests are performed for two different interference configurations (case-1 and case-2) with  $c/c$  distance-to-diameter ratios between principal and interfering chimneys of 16 and 25, respectively, for various angles of wind incidences between  $0^\circ$  and  $360^\circ$ . Figures 1 and 2 show the wind tunnel test setup for interference case-1 and case-2, respectively.

### 3 Evaluation of Modal Parameters for the Principal Chimney

Free vibration tests are performed to obtain the first natural frequency in sway mode and damping ratio of the principal chimney. Tests are conducted in two orthogonal directions by giving an initial disturbance to the aeroelastic model by hitting the model at the top using hammer. From the free vibration trace and its corresponding spectrum, natural frequency of 118 Hz is observed, and the damping ratio is computed using logarithmic decrement method which is around 1.6%. Mode shape corresponding to the first mode is obtained using measurements from two accelerometers. One accelerometer is fixed at the top of the model, and the position of the other

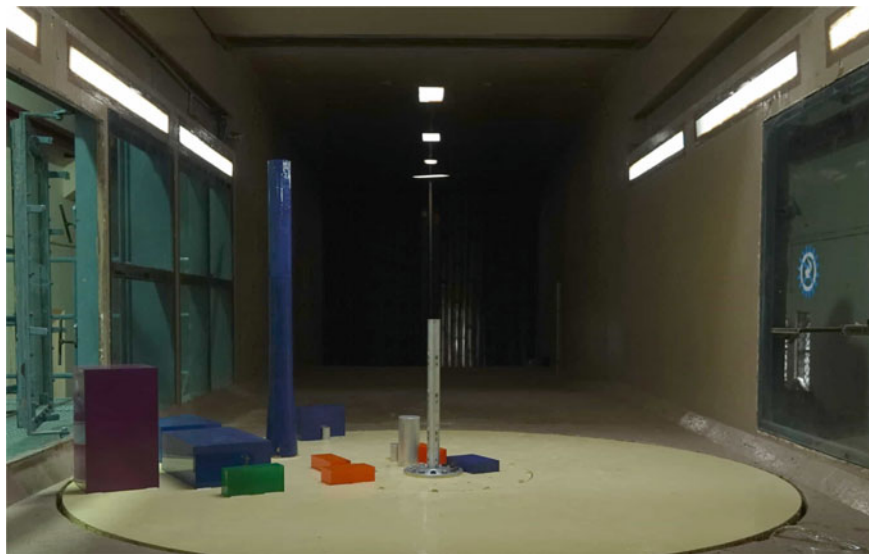


**Fig. 1** Wind tunnel setup for interference case-1 showing the principal chimney with the interfering chimney and surrounding building structures for  $120^\circ$  angle of wind incidence



**Fig. 2** Wind tunnel setup for interference case-2 showing the principal chimney with the interfering chimney and surrounding building structures for  $345^\circ$  angle of wind incidence

accelerometer is varied along the height. The relative magnitudes of spectral ordinates in the spectra of the free vibration traces of the two accelerometers at natural frequency of the model resulted in the mode shape co-ordinate at respective location along the height. Furthermore, the influence line profile for the tip deflection is evaluated by fixing a dial gauge at top of the model and varying the standard weight at different locations along the height. This influence line profile is used to compute the mean tip deflection.

## 4 Results and Discussion

### 4.1 Isolated Condition

The principal chimney is tested in stand-alone condition to understand the variation of along-wind and across-wind BMs corresponding to different wind speeds. The time histories of along-wind BMs are first resolved by separating the mean and the fluctuating components. Figure 3 shows the variation of mean and total fluctuating components of along-wind base BM with wind speeds. The values of mean BM with respect to wind speeds are found to vary linearly with square of mean wind velocity ( $U$ ). The total along-wind fluctuating component of BM is calculated using the spectra of BM and is found to linearly vary with  $U^{2.4}$ . The fitted equations using the above variations as given in Fig. 3 can be further used to compute the BMs for other wind speeds at which are not experiments are not conducted.

The across-wind BM has a zero-mean, and the time histories of across-wind BMs are converted to frequency domain to have a better understanding of the complex

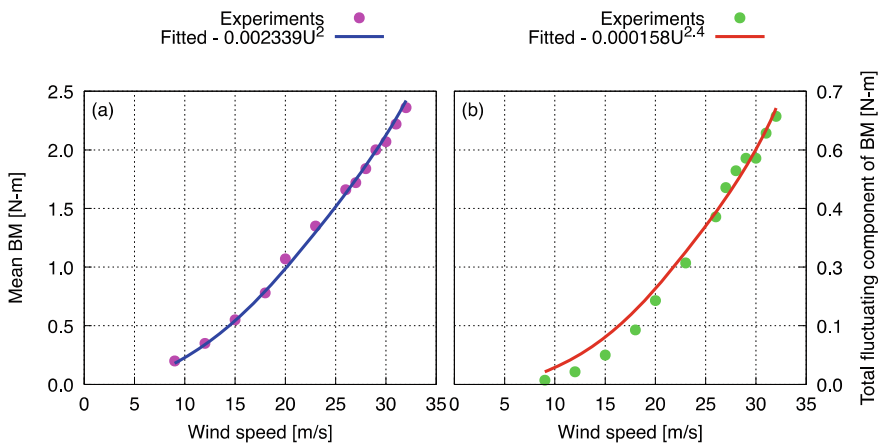


**Fig. 3** Variation of along-wind **a** mean, and **b** total fluctuation component of base BM with wind speeds

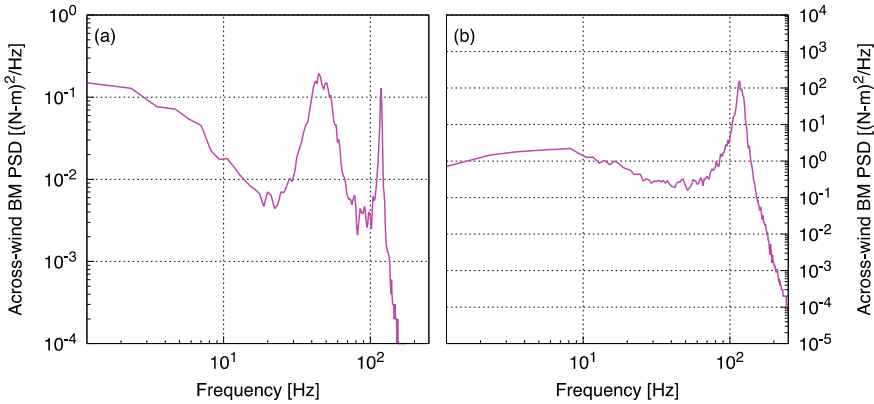


**Fig. 4** Power spectral density of across-wind BM of principal chimney in isolated condition for reduced velocities of **a** 2.38, and **b** 5.54

phenomena. Figure 4 gives the across-wind BM power spectral density (PSD) for reduced velocities of 2.38 and 5.54. At reduced velocity of 2.38, two peaks in the spectrum, one corresponding to vortex shedding frequency and other of structural frequency, are clearly observed and the Strouhal number is calculated as 0.171. It is also evident that with increase in wind speeds, there is increase in vortex shedding frequency. At reduced velocity of 5.54, there is no clear distinction between vortex shedding frequency and natural frequency in the spectrum. This clearly indicates that, at a reduced velocity of 5.54, the principal chimney is in lock-in region, where natural frequency controls the vortex shedding. The average Strouhal number considering values from all the wind speeds is computed as 0.181. Further, the critical wind speed for across-wind is evaluated as 27.15 m/s. The design wind speed for the chimney location under study is 39 m/s at top of the principal chimney, and the  $V_{z_{ref}}$  as per IS 4998:2015 [13] is 38 m/s. Since critical wind speed value is between  $0.5 V_{z_{ref}}$  and  $1.3 V_{z_{ref}}$  as mentioned in IS 4998:2015, across-wind load due to vortex shedding is critical.

### 4.2 Interference Case-1

The model of principal chimney is placed at a S/D ratio of 16 to the model of interfering chimney along with the models of surrounding structures in the corresponding locations for layout-1. Tests are conducted at different wind speeds for various wind angles of attack from  $0^\circ$  to  $360^\circ$ . Wind direction corresponding to the tandem arrangement of principal and interfering chimney is reckoned as  $0^\circ$ . All the models on the turntable are rotated in clockwise direction to conduct the tests for other angle of wind incidences. As mentioned above, as the across-wind response is critical for isolated condition, we discuss the response due to the across-wind

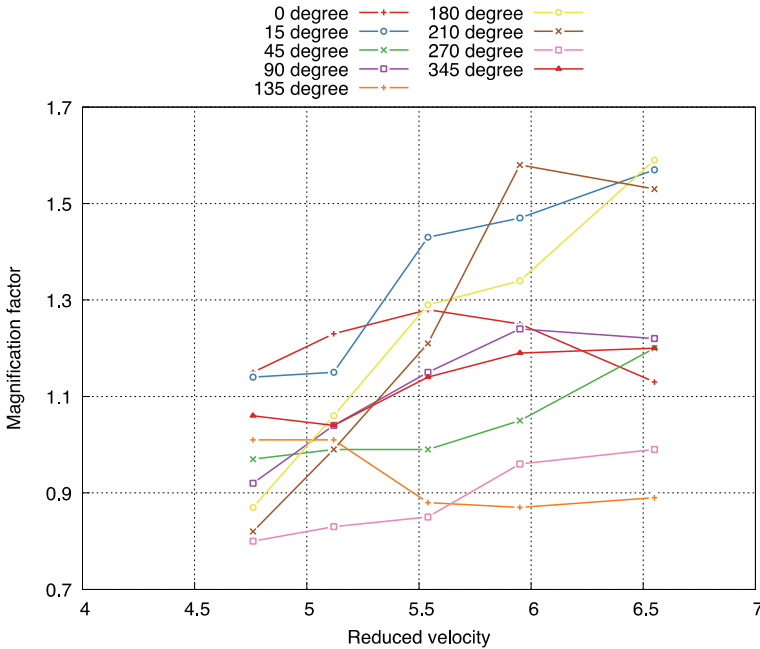


**Fig. 5** Variation of magnification factor with respect to wind speeds and wind incidence angles for interference case-1

in detail in this section for the interference cases also. Interference effects due to across-wind response are usually represented in terms of magnification factor (MF) which is defined as the ratio of the across-wind response of chimney in interference condition to the across-wind response of chimney in isolated condition. Figure 5 shows the variation of MF with respect to different wind speeds for critical angles of attack. The maximum values of MF (MMF) are observed in lock-in region for reduced velocity range of 4.75–6.55 for all the angles of attack considered. For all the test cases performed with varying wind speeds and angles of attack, MMF value of 1.6 is observed for 15°, 180° and 210°. This is also evident from Fig. 6 which shows the envelope of MMF with respect to different angles of attack.

### 4.3 Interference Case-2

For the interference case-2, the model of principal chimney is placed at a S/D ratio of 25 to the interfering chimney along with the models of other surrounding structures in the corresponding locations of the layout-2. For this case also, tests are conducted at different wind speeds and for various angles of wind incidences in the range of 0°–360° covering the critical angles related to tandem, side-by-side and staggered



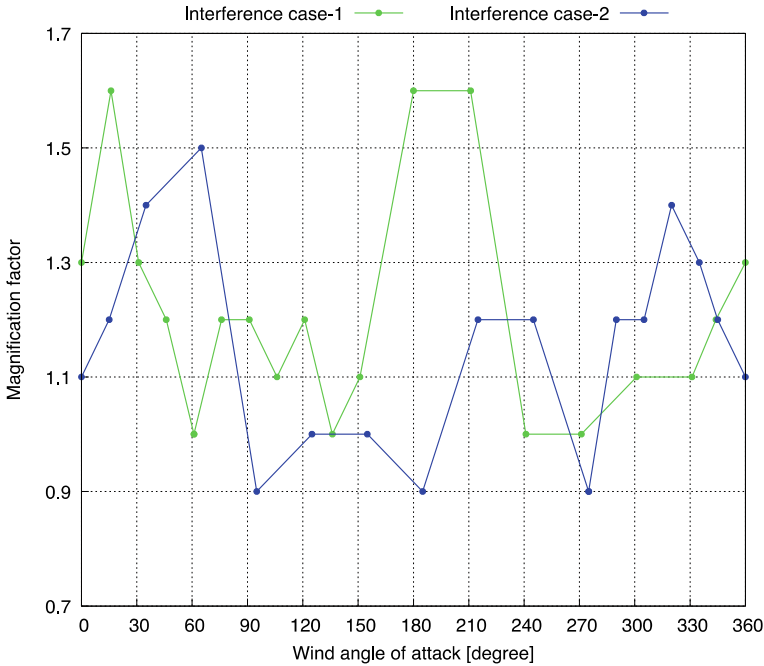


**Fig. 6** Variation of maximum magnification factor with respect to wind incidence angles for interference case-1 and case-2

arrangements. Figure 7 shows the variation of MF with respect to different wind speeds for the critical angles of wind incidences. From the envelope of MMF (Fig. 6) for the interference case-2, the maximum of MMF is observed as 1.5.

Based on the analysis of test data, the peak along-wind BM at the design wind speed of 39 m/s, for both isolated and all interference cases, is evaluated. Also, the resultant BM at critical wind speed, which is defined as the square root of the sum of squares of peak across-wind BM and mean along-wind BM at critical wind speed, is evaluated for isolated and interference cases. Resultant BM at critical wind speed is about 0.8 times its along-wind BM at design wind speed for the isolated case. For the interference cases, the ratio between resultant BM at critical wind speed and its corresponding peak along-wind BM at design wind speed for each angle of incidence is calculated. Maximum ratios of 1.25 and 1.05 are observed for case-1 and case-2, respectively. However, maximum resultant BM is 1.04 and 1.03 times the maximum peak along-wind BM from all angles of wind incidences for case-1 and case-2, respectively. From these values, it is clearly evident that the interference effects are predominant in both along-wind and across-wind directions depending upon the angle of wind incidence.

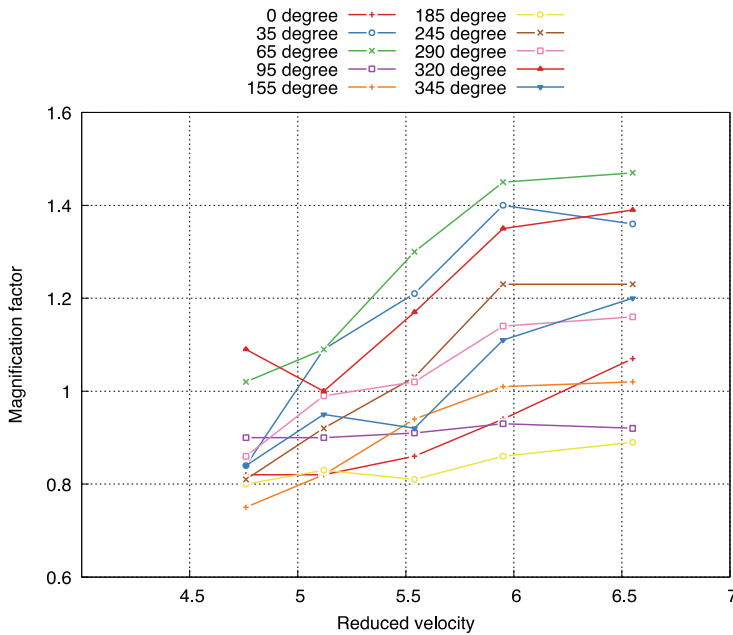


**Fig. 7** Variation of magnification factor with respect to wind speeds and wind incidence angles for interference case-2

## 5 Conclusion

Wind-induced interference effects on a 125 m tall chimney due to the presence of surrounding structures including a 275 m tall chimney for two different interference cases are assessed using wind tunnel studies. Experimental setup and results are briefly discussed in this paper. The results pertaining to BM at base are only discussed. The maximum values of the MF from the envelope of the MMF are observed as 1.6 and 1.5 for case-1 and case-2, respectively. Interference effects are predominant in both along-wind and across-wind directions depending upon the angle of wind incidence for the tested interference configurations. The paper presents only case study related to specific configurations. In addition to this specific study, systematic investigations are needed to establish the individual roles of the location of 275 m tall chimney and other surroundings structures as a whole in creating group effects.

## References

1. Zdravkovich M (1987) The effects of interference between circular cylinders in cross flow. *J Fluids Struct* 1(2):239–261
2. Gowda BL, Sreedharan V, Narayanan S (1993) Vortex induced oscillatory response of a circular cylinder due to interference effects. *J Wind Eng Ind Aerodyn* 49(1–3):157–166
3. Kareem A, Kijewski T, Lu PC (1998) Investigation of interference effects for a group of finite cylinders. *J Wind Eng Ind Aerodyn* 77:503–520
4. Gu Z, Sun T (1999) On interference between two circular cylinders in staggered arrangement at high subcritical Reynolds numbers. *J Wind Eng Ind Aerodyn* 80(3):287–309
5. Liu X, Levitan M, Nikitopoulos D (2008) Wind tunnel tests for mean drag and lift coefficients on multiple circular cylinders arranged in-line. *J Wind Eng Ind Aerodyn* 96(6–7):831–839
6. Niemann HJ, Kasperski M (1999) Interference effects for a group of two reinforced concrete chimneys. *J Fluids Struct* 13(7–8):987–997
7. John AD, Gairola A, Ganju E, Gupta A (2011) Design wind loads on reinforced concrete chimney—an experimental case study. *Procedia Eng* 14:1252–1257
8. Sun Y, Li Z, Sun X, Su N, Peng S (2020) Interference effects between two tall chimneys on wind loads and dynamic responses. *J Wind Eng Ind Aerodyn* 206:104227
9. Su N, Li Z, Peng S, Uematsu Y (2021) Interference effects on aeroelastic responses and design wind loads of twin high-rise reinforced concrete chimneys. *Eng Struct* 233:111925
10. ACI 307 (2008) Code requirements for reinforced concrete chimneys (ACI 307-08) and commentary. American Concrete Institute Farmington Hills
11. Rajora R, Veeravalli SV, Ahmad S (2020) Aerodynamic interference of straight and tapered cylinder pairs near the first critical wind speed. *J Wind Eng Ind Aerodyn* 201:104171
12. IS 875 (Part 3) (2015) Code of practice for design loads (other than earthquake) for buildings and structures, Part 3. Bureau of Indian Standards, New Delhi
13. IS 4998 (2015) Criteria for design of reinforced concrete chimneys. Bureau of Indian Standards, New Delhi